

Measurement of Long-Range Repulsive Forces between Charged Particles at an Oil-Water Interface

R. Aveyard, B. P. Binks, J. H. Clint, P. D. I. Fletcher,* T. S. Horozov, B. Neumann, and V. N. Paunov
Surfactant & Colloid Group, Department of Chemistry, University of Hull, Hull HU6 7RX, United Kingdom

J. Annesley, S. W. Botchway, D. Nees, A. W. Parker, and A. D. Ward
CLRC, Rutherford Appleton Laboratory, Chilton, Didcot, Oxon OX11 0QX, United Kingdom

A. N. Burgess
ICI PLC, P.O. Box 90, Wilton Centre, Middlesborough, Cleveland TS90 8JE, United Kingdom
 (Received 11 October 2001; published 3 June 2002)

Using a laser tweezers method, we have determined the long-range repulsive force as a function of separation between two charged, spherical polystyrene particles ($2.7\ \mu\text{m}$ diameter) present at a nonpolar oil-water interface. At large separations (6 to $12\ \mu\text{m}$ between particle centers) the force is found to decay with distance to the power -4 and is insensitive to the ionic strength of the aqueous phase. The results are consistent with a model in which the repulsion arises primarily from the presence of a very small residual electric charge at the particle-oil interface. This charge corresponds to a fractional dissociation of the total ionizable (sulfate) groups present at the particle-oil surface of approximately 3×10^{-4} .

DOI: 10.1103/PhysRevLett.88.246102

PACS numbers: 68.05.Gh, 41.20.Cv, 42.50.Vk, 82.70.Dd

We have used a laser tweezers method to investigate the very long-range repulsive forces which have recently been observed to operate between particles present in monolayers at the nonpolar oil-water interface [1]. Such forces have general relevance to the properties of emulsions stabilized by adsorbed solid particles. Interparticle repulsion leads to high order in relatively dilute monolayers; an image of a monolayer of spherical polystyrene latex particles at the interface between water and a mixture of decane and undecane is shown in Fig. 1. The particles, which carry ionizable sulfate groups at their surfaces, have a diameter of $2.7\ \mu\text{m}$.

It has been shown [2,3] that the electrostatic repulsion between charged particles at an interface between water and a medium of low relative permittivity (air or oil) is enhanced over that between similar particles in bulk water. The origin of the effect is due to the asymmetry of the electrical double layer at that part of the particle surface in the aqueous phase, which gives rise to an effective dipole normal to the liquid surface. The dipole-dipole repulsion through the phase of low relative permittivity is longer range than that through the aqueous (electrolyte) phase, the latter being subject to counterion screening. Theoretical treatments of the phenomenon have subsequently been given by Hurd [4], by Earnshaw [5], and by Goulding and Hansen [6].

It has been demonstrated [1], however, that the “long range” repulsion arising from asymmetric double layers of adsorbed particles is insufficient to give rise to the kind of structuring seen in Fig. 1. The ultralong range repulsion between polystyrene particles has been attributed to a small amount of surface electric charge present at the oil/particle interface. We believe that this charge originates from the surface sulfate groups, a very small fraction

of which is stabilized by water trapped on the rough particle surface. The interparticle repulsion between two particles is thought to arise from unscreened charge-charge interactions acting through the oil phase together with interactions involving the charge on one particle and the image charge (in the water phase) of the other particle. Importantly, the repulsion between particles at the oil/water interface is insensitive to the presence of even high concentrations of electrolyte ($1\ \text{mol dm}^{-3}$) in the aqueous phase. This observation is contrary to the predictions of the interparticle forces based on dipole-dipole interactions which

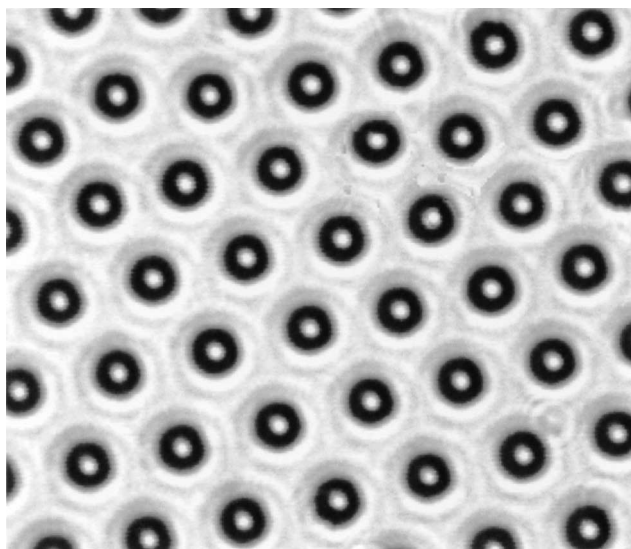


FIG. 1. Optical micrograph of a monolayer of polystyrene spheres, diameter $2.7\ \mu\text{m}$, at the interface between water and a mixture of decane and undecane in the trough (see Fig. 2); the average distance between particle centers is $5.8\ \mu\text{m}$. In the force experiments much more dilute films have been used.

are expected to decrease strongly when the ionic strength of the aqueous phase is increased [4]. Most recently Sun and Stirner have carried out molecular dynamics simulations of charged colloidal monolayers, and included finite size effects in their analysis [7]. They conclude that the long-range repulsion is mainly controlled by charge-charge interactions.

Direct measurements of the interaction potentials between two charged colloidal particles in the bulk of an aqueous suspension have been made as a function of particle separation by Crocker and Grier using an optical tweezers method [8]. We report in this Letter the first measurements using optical tweezers of the forces between a pair of charged polystyrene spheres (diameter $2.7 \mu\text{m}$), trapped at the interface between an alkane mixture and water, as a function of the particle separation.

The polystyrene particle monolayers (see Fig. 1) were obtained by spreading the particles from a dispersion in a mixture of (mainly) isopropanol and water (300:1 by volume, respectively), at the interface between water and a mixture of decane (70.5 vol %) and undecane (29.5 vol %) in a small polytetrafluorethylene (PTFE) trough (see Fig. 2). The particles were monodisperse ($2.7 \mu\text{m}$ diameter) and had a surface charge density, arising from the terminal sulfate groups, of $8.9 \mu\text{C cm}^{-2}$ (value supplied by the particle manufacturer Interfacial Dynamics Corp., USA). Force measurements were made for aqueous phases of either pure water (ionic strength $\approx 3 \times 10^{-6} \text{ M}$) or water containing 1 mM NaCl. The composition of the oil phase was chosen in order to match its viscosity to that of water. Monolayers used in the force measurements were much more dilute than in the system depicted in Fig. 1.

A complete description of the laser tweezers apparatus is given in Ref. [9]. The trough containing the spread monolayer was mounted on the stage of a Leica DM IRB inverted microscope. A variable power continuous wave Nd:YAG laser, operating at wavelength 1064 nm, entered

the trough from below and was focused by the microscope objective ($40\times$ magnification, numerical aperture 0.5, working distance 2 mm). The trap was formed at the waist of the beam focus located in the plane of the oil/water interface. The trough containing the monolayer is illustrated in Fig. 2. In the present configuration the single laser was employed to create two traps using fast response acousto-optic deflection (AOD). Each trap had a “dwell time” of 1 ms at each trap position with a transit time of $6 \mu\text{s}$. The separation between the two traps was adjustable using computer control of the AOD. The microscope stage was equipped with piezoelectric translators which enabled computer controlled lateral movement of the stage, and hence of the monolayer in the trough. The particles in the monolayer were observed using a CCD camera, attached to the microscope, with fast frame image acquisition for subsequent analysis. All measurements were made at 21°C .

Using a set laser power, P , two particles in the monolayer were trapped initially at a large separation. The separation was decreased to determine the separation at which one of the particles was released from a trap; this gives the interparticle force that is equal to the trapping force at the laser power P . This procedure was repeated for a range of values of P . The measured P values were converted to forces using the calibration method now to be described, and hence the force-distance relationship for two particles was obtained. In order to obtain the relationship between force f and laser power P , two particles were trapped at large separation ($19 \mu\text{m}$) such that their mutual interaction was negligible. A lateral oscillatory movement was then applied to the stage in a direction normal to the line between the trapped particle centers in order to create a velocity dependent viscous drag force on the particles. The stage movement had a smoothed triangular waveform, with a total displacement amplitude of $72 \mu\text{m}$. The maximum stage velocity, v_{max} , was varied by adjustment of the frequency of the triangular waveform. The maximum (critical) value of v_{max} , v_{max}^* , just sufficient to free the particles from the traps, was determined for each value of P . The drag force is related to v_{max}^* by

$$f \approx 6\pi\eta R v_{\text{max}}^*, \quad (1)$$

where η is the viscosity of the liquid (matched for the oil and water phases) and R is the particle radius. Equation (1) is only approximate since the presence of the oil-water interface perturbs the flow streamlines. However, from symmetry arguments it is expected to be valid in the case where the contact angle, θ , of the particle with the oil-water interface is 90° . The observed contact angle measured through the water phase (when the oil phase is octane) for similar particles is $75 \pm 5^\circ$ [1]. Although the problem of the drag coefficient of a particle in a liquid-liquid interface has not been solved yet, the case of particles at a liquid-gas interface has been considered theoretically [10]. Based on the results of this work, it is estimated that the use of the approximate Eq. (1)

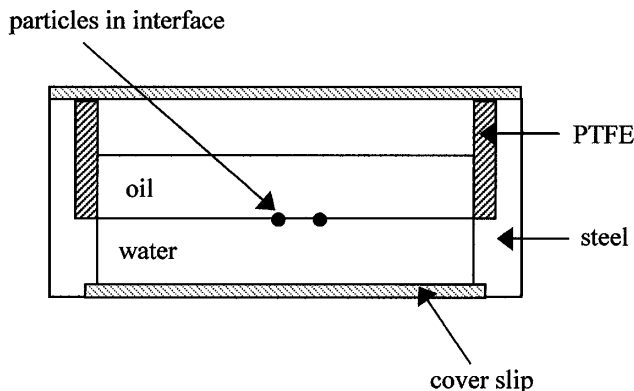


FIG. 2. Side view of the circular trough, internal diameter 25 mm. Pinning of the oil-water interface at the steel-PTFE junction enables the formation of a flat interface.

leads to an underestimation of the absolute magnitude of the drag force with a systematic error of less than 10%, similar to the experimental uncertainties in the measured forces. The results of the calibration are illustrated in Fig. 3, where plots of v_{\max}^* against P (filled points) and the corresponding f against P (open points) are shown.

The measured interparticle force, f_{inter} , is depicted in Fig. 4 as a function of separation, L , between the centers of particles for aqueous phases containing either zero added electrolyte (ionic strength $\approx 3 \times 10^{-6}$ M) or 1 mM NaCl. It can be seen that the force scales as L^{-4} and is insensitive to the ionic strength of the aqueous phase. The experimental results are compared with two alternative theories. According to Stillinger [2], Pieranski [3], and Hurd [4], the long-range repulsion corresponds to an effective dipole-dipole interaction resulting from the asymmetry of the particle ionic atmosphere in water due to the presence of the particle/oil interface. Using Hurd's theory, taking into account the difference in relative dielectric constant of air and oil and the finite particle size, the force is

$$f_{\text{inter}} \approx \frac{6\epsilon_{\text{oil}}q_{\text{water}}^2}{4\pi\epsilon_0\epsilon_{\text{water}}^2\kappa^2L^4}, \quad (2)$$

where ϵ_0 is the permittivity of free space, ϵ_{oil} and ϵ_{water} are the relative dielectric constants of oil and water, respectively, q_{water} is the charge of the water-immersed section of the particle, and κ^{-1} is the Debye screening length. When $\kappa R \ll 1$, $q_{\text{water}} = 2\pi R^2(1 + \cos\theta)\sigma\alpha_{\text{water}}$, where σ is the particle surface charge density corresponding to full dissociation and α_{water} is the degree of dissociation of the sulfate groups at the particle-water surface. However, in our experiment, $\kappa R \gg 1$; i.e., only the particle surface charges within a distance κ^{-1} from the three-phase con-

tact line effectively contribute to the long-range particle-particle interaction. The rest of the particle surface charge in water is screened similarly as in the bulk of the electrolyte and gives only a short-range (Debye-Hückel type) contribution to the interaction force. Thus, the effective value of the particle/water surface charge to be accounted for in Eq. (2) is $q_{\text{water}} = 2\pi R \sin\theta \kappa^{-1} \sigma \alpha_{\text{water}}$. In this case

$$f_{\text{inter}} \approx \frac{24\pi^2 R^2 \sin^2\theta \epsilon_{\text{oil}} \sigma^2 \alpha_{\text{water}}^2}{4\pi \epsilon_0 \epsilon_{\text{water}}^2 \kappa^4 L^4}. \quad (3)$$

Equation (3) predicts that the expected force contribution from this effect should scale with κ^{-4} , corresponding to an inverse square scaling with the ionic strength of the aqueous phase. This scaling is not observed in the results of Fig. 4 where it can be seen that the force is the same for pure water (ionic strength approximately 3×10^{-6} M) and 1 mM NaCl. The dashed line of Fig. 4 shows the force calculated using Eq. (3) with the following known values for the parameters: $R = 1.35 \mu\text{m}$, $\theta = 75^\circ$, $\sigma = 8.9 \mu\text{C cm}^{-2}$, $\epsilon_{\text{oil}} = 2$, and ionic strength = 3×10^{-6} M (pure water). The unknown value of α_{water} was taken to be 0.25, typical of the values for ionic micelles of similar surface charge density. Hence, even for pure water, the calculated force is small compared to the experimental values. At higher ionic strengths, the calculated force is insignificant.

The solid curve of Fig. 4 was calculated according to the model presented by Aveyard *et al.* [1] in which the dominant repulsive force is postulated to occur as a result

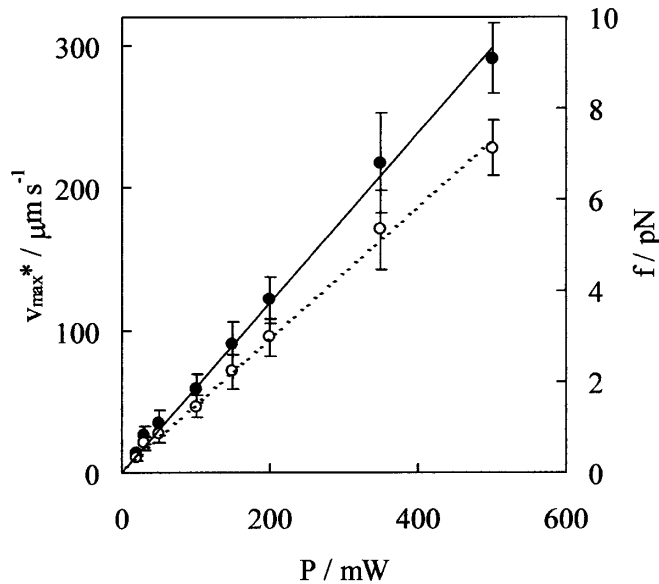


FIG. 3. Laser trap calibration plot showing v_{\max}^* versus laser power P (left-hand ordinate, filled symbols) and the corresponding values of trap force f (right-hand ordinate, open symbols).

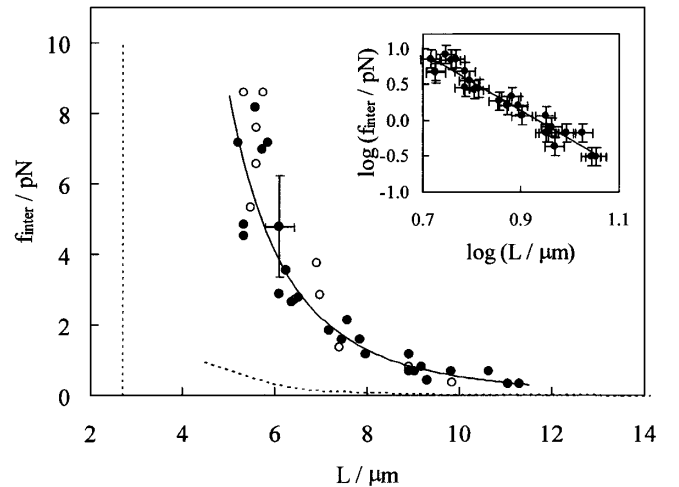


FIG. 4. Interparticle repulsive force versus center-to-center particle separation for aqueous phases containing zero added electrolyte (filled circles) and 1 mM NaCl (open circles). The vertical dashed line corresponds to contact of the particle surfaces. The curved dashed line is calculated using Eq. (3) with κ corresponding to pure water and $\alpha_{\text{water}} = 0.25$. The solid curve is calculated using Eq. (5) with the parameters given in the text. The inset shows a double logarithmic plot for the system with zero added electrolyte, for which the best-fit slope is -4.0 ± 0.5 for a confidence level of 95%.

of the presence of a small amount of net charge at the particle-oil surface. This charge is represented by a point charge, q_{oil} , located at a distance ζ above the oil-water interface and is given by the product of the particle surface area immersed in the oil, the surface charge density σ and the fractional degree of dissociation, α_{oil} , of the ionizable groups at the oil-particle interface. Thus

$$q_{oil} = 2\pi R^2 \sigma (1 - \cos\theta) \alpha_{oil}. \quad (4)$$

The interaction force between particles is obtained by differentiation of Eq. A23 in Ref. [1],

$$f_{inter} \approx \frac{q_{oil}^2}{4\pi \epsilon_{oil} \epsilon_0} \left\{ \frac{1}{L^2} - \frac{L}{(4\zeta + L^2)^{3/2}} \right\}. \quad (5)$$

The value of ζ is given by [1]

$$\zeta = R(3 + \cos\theta)/2. \quad (6)$$

The first term in Eq. (5) corresponds to the Coulombic interaction between two identical point charges, of magnitude q_{oil} , across the oil phase. The second term corresponds to the interaction between the second particle, charge q_{oil} , and the image charge of the first particle. At large separations such that $(\zeta/L)^2 \ll 1$, the interaction has the asymptotic form expected for a charge-dipole interaction

$$f_{inter} \approx \frac{6q_{oil}^2 \zeta^2}{4\pi \epsilon_{oil} \epsilon_0 L^4}. \quad (7)$$

In agreement with Eqs. (5) and (7), the measured force is independent of the ionic strength of the aqueous phase and decays as L^{-4} , as shown in the inset log-log plot in Fig. 4, the slope of which is -4.0 ± 0.5 for a confidence level of 95%. The solid curve of Fig. 4 was obtained by using the known values for the parameters quoted above. The unknown value of the degree of dissociation α_{oil} was floated to obtain the best-fit value, which was found to be 3.3×10^{-4} . Within the precision of the data, the model accounts reasonably well for the experimentally measured interparticle forces, both for pure water and for 1 mM NaCl. The value of α obtained here (3.3×10^{-4}) is significantly smaller than the values of 0.01 [1] estimated by fitting the model described above to surface pressure data for similar particles at the octane-water interface. We be-

lieve that the observed difference results from the effect on surface pressure (measured at a lower range of particle separations than the force measurements described here) of surface active oligomers leached from the latex particles by the spreading solvent (isopropanol).

Additional experiments (results not shown) were made with similar latex particles of radius $1.95 \mu\text{m}$ and $\sigma = 7.5 \mu\text{C cm}^{-2}$ with pure water. The forces, again found to scale as L^{-4} , were approximately twofold higher than those for the $1.35 \mu\text{m}$ particles shown in Fig. 4. The observed force increase is less than that predicted from Eq. (5) if it assumed that both θ and α_{oil} are equal for the two particle types. The forces measured for the larger particles are consistent with Eq. (5) if either θ is taken to be 55° (compared with 75° measured for the small particles) or α_{oil} is taken to be 2×10^{-4} (compared with 3.3×10^{-4} estimated for the small particles).

The main conclusions from this study are that charged polymer particles adsorbed at the oil-water interface exhibit a long-range repulsive force which scales as separation distance to the power -4 and is insensitive to the electrolyte content of the aqueous phase. The results are consistent with a model in which the repulsion arises primarily from the presence of a small residual electric charge at the particle-oil interface.

We thank ICI, Wilton, the Central Laser Facility, CLRC, and the Engineering and Physical Sciences Research Council for financial support.

*Corresponding author.

Email address: P.D.Fletcher@hull.ac.uk

- [1] R. Aveyard, J. H. Clint, D. Nees, and V. N. Paunov, *Langmuir* **16**, 1969 (2000).
- [2] F. H. Stillinger, *J. Chem. Phys.* **35**, 1584 (1961).
- [3] P. Pieranski, *Phys. Rev. Lett.* **45**, 569 (1980).
- [4] A. J. Hurd, *J. Phys. A* **18**, L1055 (1985).
- [5] J. C. Earnshaw, *J. Phys. D* **19**, 1863 (1986).
- [6] D. Goulding and J-P. Hansen, *Mol. Phys.* **95**, 649 (1998).
- [7] J. Sun and T. Stirner, *Langmuir* **17**, 3103 (2001).
- [8] J. C. Crocker and D. G. Grier, *Phys. Rev. Lett.* **77**, 1897 (1996).
- [9] D. Nees, S. W. Botchway, M. Towrie, A. D. Ward, A. W. Parker, and A. Burgess, Central Laser Facility, Rutherford Appleton Laboratory, Annual Report No. 209, 1999/2000.
- [10] K. Danov, R. Aust, F. Durst, and U. Lange, *J. Colloid Interface Sci.* **175**, 36 (1995).